

## Circulation on the shelf and the upper slope of the Bay of Biscay

Arnaud Le Boyer<sup>a,\*</sup>, Guillaume Charria<sup>a</sup>, Bernard Le Cann<sup>b</sup>, Pascal Lazure<sup>a</sup>, Louis Marié<sup>c</sup>

<sup>a</sup> DYNECO-Physed, Ifremer, Centre de Bretagne, BP 70, 29280 Plouzané, France

<sup>b</sup> Laboratoire de Physique des Océans, UMR6523 UBO-CNRS-IRD-IFREMER, Université de Bretagne Occidentale, 6, Avenue Le Gorgeu, Brest, 29238 France

<sup>c</sup> Laboratoire de Physique des Océans, UMR6523 UBO-CNRS-IRD-IFREMER, Ifremer, Centre de Bretagne, BP70, 29280 Plouzané, France

\*: Corresponding author : Arnaud Le Boyer, tel.: +33298224330 ; email address : [arnaud.leboyer@ifremer.fr](mailto:arnaud.leboyer@ifremer.fr)

### Abstract:

Here, we used measurements taken with an array of 10 acoustic Doppler current profilers deployed from July 2009 to August 2011 to describe the tidally filtered circulation over the shelf and upper slope on the French side off the French coasts of the Bay of Biscay. The measurements provided an overview of the shelf and slope circulation throughout the entire water column over a large range of spatial and time scales. The average circulation over the shelf and upper slope of the Bay of Biscay was poleward following the topography with a speed of the order of  $3 \text{ cm s}^{-1}$ . This average circulation had marked seasonal variability. In summer, the currents were equatorward on the outer shelf near surface. Deeper in the water column, the flow remained poleward. In winter, the intensity of the current increased in the north, while it reached its maximum in the south in autumn. On a weekly scale, this behaviour was associated with strong surface currents near the coast in the northern part of the domain in winter and strong currents affected the whole water column in the southern part of the domain in autumn. Correlations of the along-shore currents with wind suggest that wind stress drives almost half of the total observed circulation. We suggest that this forcing acts either directly via local winds or potentially by coastal-trapped waves generated by non-local winds. The potential remote forcing mechanism acts predominately in the southern Bay of Biscay when the wind blows eastward along the northern Spanish coast.

### Highlights

► Two years time series of the current in the water column from Penmarc'h to Capbreton. ► Strong surface current near Penmarc'h in winter. ► Barotropic strong currents close to Capbreton canyon for the autumn. ► A part of the variability close to the Capbreton canyon is remotely forced.

**Keywords:** Bay of Biscay ; Observation ; Shelf and slope circulation ; Vertical profile ; ADCP ; Wind driven circulation

### 1. Introduction

The continental shelf of the Bay of Biscay (BoB) west of France is located in the eastern part of the Atlantic Ocean between Capbreton Canyon and Penmarc'h Point (Fig. 1). One feature of the BoB is the northward widening of the shelf. From the Spanish coast to Penmarc'h Point, the width of the continental shelf varies from  $\sim 60 \text{ km}$  to  $\sim 160 \text{ km}$  in front of the Loire River. This study focuses on the circulation on the shelf and the upper part of the continental slope. The continental slope is irregular and has many promontories and canyons (Fig. 1). The first large-scale studies of the area were hydrological (e.g. Vincent and Kurc, 1969a; Le Cann, 1982, Le Cann, 1988 and Puillat et al., 2004). They show a seasonal (from spring to autumn) bottom-trapped water mass with a temperature of  $12 \text{ }^\circ\text{C}$  between the 60 m and 120 m isobaths. This so-called "bourrelet froid" (cold pool) appears after the seasonal thermocline sets up, insulating the bottom water

1  
2  
3  
4  
5 Such a pattern can also be observed in other regions like the Irish sea (Brown  
6 et al., 2003) and over the Mid-Atlantic Bight (Houghton et al., 1982). The  
7 surface temperatures vary from  $10^{\circ}C$  in the north in winter to  $> 21^{\circ}C$  in  
8 the south in summer. With the exception of winter, the thermocline depth is  
9 close to the depth of the  $12^{\circ}C$  isotherm at  $\sim 40$  meters depth in spring and  
10  $\sim 70$  meters depth in autumn. In winter, the water masses are homogeneous  
11 on the vertical.  
12

13  
14  
15  
16  
17  
18 Despite its complex topography, this area features a classical eastern  
19 boundary current system exhibiting a poleward flow on the shelf and slope  
20 (Koutsikopoulos and Le Cann, 1996) and is influenced by the eastern edge  
21 of the large scale oceanic basin circulation (Pollard and Pu, 1985). These  
22 open ocean boundary conditions force the slope current to be unstable and  
23 generate eddies observed in the interior of the BoB. In addition, they can act  
24 in concert with the wind and the buoyancy gradient to drive shelf circulation.  
25  
26  
27  
28  
29  
30

31 The complex circulation of the BoB has been studied for several years with  
32 in situ data. Over the abyssal plain, the average circulation shows a very weak  
33 ( $1-2 \text{ cm s}^{-1}$ ) anticyclonic trend (Pingree, 1993). However, the circulation  
34 is affected by mesoscale dynamics. Anticyclonic eddies called SWODDies  
35 (Pingree and Le Cann, 1992) are generated on the slope of the BoB. The  $\star$   
36 generation of these eddies influences the circulation of the open and coastal  
37 ocean. The slope current was documented by Pingree and Le Cann (1990)  
38 who used available current meter data to establish its flow at a mean speed of  
39  $5-10 \text{ cm s}^{-1}$ . This current is highly seasonal and geographically influenced.  
40  
41  
42  
43  
44  
45  
46  
47  
48  
49  
50  
51  
52  
53  
54  
55  
56  
57  
58  
59  
60  
61  
62  
63  
64  
65

1  
2  
3  
4  
5 depth) observed from drifters over the last 17 years. The amount of drifter \*  
6 data allows an accurate description of the surface circulation. It shows mean  
7 poleward circulation on the slope and a strong seasonal variability on the  
8 shelf. For spring and summer, the surface circulation, on the French side of  
9 the BoB Shelf and Slope (hereafter, BoBSS), is equatorward while in winter  
10 and autumn, at the surface, water masses flow poleward. The circulation  
11 in the BoB is strongly influenced by the seasonal variation of wind (Pingree  
12 and Le Cann, 1989), heat fluxes (Somavilla et al., 2012) and freshwater inflow  
13 (Lazure and Jegou, 1998; Lazure et al., 2008; Ferrer et al., 2009).  
14  
15  
16  
17  
18  
19  
20  
21

22 To improve our knowledge of the circulation in the BoBSS, the objective  
23 of the ASPEX experiment was to observe the shelf and upper continental  
24 slope circulation through the water column over large spatial and temporal  
25 ranges. This study focuses on the seasonal dynamics and the horizontal  
26 velocities observed over 2 years from July 2009 to August 2011. In section  
27 2, we describe the scientific project which provides the current data and the  
28 numerical model which we use to discuss the wind driven circulation. In  
29 section 3, we present a seasonal analysis of the wind regime and the observed  
30 circulation in the BoB using different time scales. Then, we discuss in section  
31 4 the influence of the wind on the observed circulation in the BoB and other  
32 mechanisms which also drive the circulation. We conclude our work in section  
33 5.  
34  
35  
36  
37  
38  
39  
40  
41  
42  
43  
44  
45  
46  
47  
48  
49  
50  
51  
52  
53  
54  
55  
56  
57  
58  
59  
60  
61  
62  
63  
64  
65

## 2. Data and Methods

### 2.1. ASPEX Experiment

During the ASPEX project, ten current-meter moorings are deployed over the shelf and the upper part of the slope of the BoB from July 2009 to August 2011. They are organized in three sections (see Figure 1). Moorings 1, 2, 3 constitute the "Penmarc'h section". Moorings 4, 5, 6 compose the "Loire section". The last section along  $44^\circ$  N, north of the Capbreton canyon is called the " $44^\circ$ N section" with moorings 7, 8, 9 and 10. Each section is instrumented along 3 isobaths with RDI WorkHorse Acoustic Doppler Currents Profilers (ADCP):  $\sim 450$  m isobath (moorings 3, 6, 10) with ADCP operating at 75 kHz,  $\sim 130$  m isobath (mooring 2, 5, 9) with ADCP operating at 150 kHz and the  $\sim 60$  m isobath (moorings 1, 4, 7) with ADCP operating at 300 kHz. Mooring 8 is an ADCP operating at 300 kHz but it is deployed on the 70 m isobath. It needs to be noted that the ADCPs are not deployed exactly on the 450 m, 130 m, 70 m and 60 m isobaths but for the sake of simplicity, we use these isobaths for the description of the results and the discussion. The moorings are all swivel-mounted on a frame together with an SBE37 Microcat T/S/P recorder. One difficulty concerning the organization of experiments in this area is the dense fishing activity which can lead to ADCP damage. Special care was taken to detect irregularities in the pressure time series during the recording associated with trawl contact. These error sources were removed from the data and linearly fitted to fill the gaps in the time series. Figure 2 presents the recording time for each mooring after removing the outlier data. We can see that missing data are located mainly in the Loire section at the 130 m isobath (mooring 5) and in

1  
2  
3  
4  
5  
6  
7  
8  
9  
10  
11  
12  
13  
14  
15  
16  
17  
18  
19  
20  
21  
22  
23  
24  
25  
26  
27  
28  
29  
30  
31  
32  
33  
34  
35  
36  
37  
38  
39  
40  
41  
42  
43  
44  
45  
46  
47  
48  
49  
50  
51  
52  
53  
54  
55  
56  
57  
58  
59  
60  
61  
62  
63  
64  
65

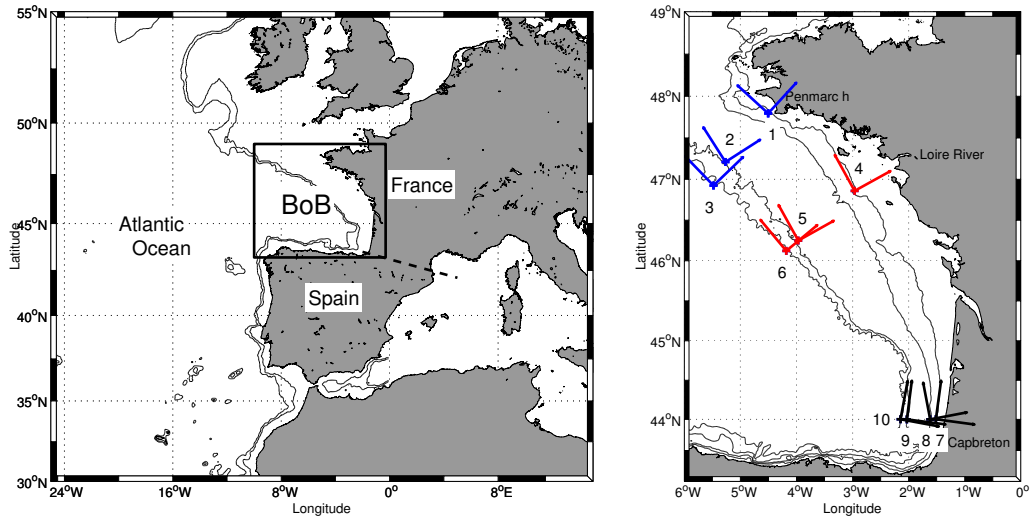


Figure 1: a): Bay of Biscay (BoB) geographical location in the North Atlantic Ocean. b) Mooring positions in the ASPEX project. The numbers are the ASPEX moorings nomenclature. Blue: Penmarc'h section. Red: Loire Section. Black: 44°N section. Thin black lines show 60, 100, 130 and 450 m isobaths. The vectors denote the along-shore and cross-shore directions obtained using the Empirical Orthogonal Function method (see text)

the 44°N section at the 70 m isobath (mooring 8).

1  
2  
3  
4  
5  
6  
7  
8  
9  
10  
11  
12  
13  
14  
15  
16  
17  
18  
19  
20  
21  
22  
23  
24  
25  
26  
27  
28  
29  
30  
31  
32  
33  
34  
35  
36  
37  
38  
39  
40  
41  
42  
43  
44  
45  
46  
47  
48  
49

7

		Penmarc'h			Loire		
	Mooring Number	1	2	3	4	5	6
	Latitude (N)	47°48'	47°13'	46°55'	46°52'	46°15'	46°07'
	Longitude (W)	-4°30'	-5°16'	-5°29'	-2°58'	-3°58'	-4°11'
	Cell size (m)	2	8	16	2	8	16
	Sound Frequency (kHz)	300	150	75	300	150	75
	Sampling Period (s)	30	30	150	30	30	150
	Mooring Depth (m)	71	130	453	52	135	423
2009 2010	Start	2009/07/13	2009/07/13	2009/07/14	2009/07/15	2009/07/16	2009/07/16
	End	2010/05/13	2010/05/14	2010/05/14	2010/06/29	2009/12/16	2010/05/18
	Duration (days)	303	304	304	349	152	306
2010 2011	Mooring Depth (m)	71	138	457	47	135	416
	Start	2010/08/31	2011/02/02	2010/09/01	2010/09/02	2010/09/03	2010/09/03
	End	2011/08/07	2011/06/25	2011/08/08	2011/08/09	2011/01/06	2011/08/13
	Duration (days)	341	143	341	341	125	344
		44° N					
	Mooring Number	7	8	9	10		
	Latitude (N)	44°00'	44°00'	44°00'	44°00'		
	Longitude (W)	-1°31'	-1°34'	-2°02'	-2°09'		
	Cell size (m)	2	2	8	16		
	Sound Frequency (kHz)	300	300	150	75		
	Sampling Period (s)	30	30	30	150		
	Mooring Depth (m)	54	71	138	456		
2009 2010	Start	2009/07/19	2009/07/19	2009/07/18	2009/07/18		
	End	2010/06/29	2009/10/31	2010/07/01	2010/03/29		
	Duration (days)	327	104	347	253		
2010 2011	Mooring Depth (m)	54	71	134	454		
	Start	2010/09/05	2011/02/06	2010/09/04	2010/09/05		
	End	2011/08/10	2011/08/10	2011/07/11	2011/08/10		
	Duration (days)	338	184	309	339		

Table 1: ASPEX Moorings characteristics

1  
2  
3  
4  
5 Table 1 presents the characteristics of the recorded data from the 10  
6 ADCPs located on the shelf and the upper part of the slope of the BoB for the  
7 year 2009/2010 and the year 2010/2011. The mooring depth represents the  
8 time average of the pressure recorded by the instruments converted to meters.  
9 Depending on the instrumented isobath, the cell size of the observations  
10 is 2 meters, 8 meters and 16 meters for the 60, 130 and 450 m isobaths,  
11 respectively. The deepest cell which records the current is located above the  
12 ADCP at a height of about one and a half cell size. The ADCP beam angle  
13 is  $20^\circ$  to the vertical. Due to the beam angle, the reflection of sound at the  
14 surface contaminates cells close to the surface. Thus, only  $\sim 80\%$  (from the  
15 deepest cell to the shallowest cell) of the total water column can be sampled.  
16 The sampling period is 30 s for both the 300kHz and 150kHz ADCPs and  
17 150 s for the 75kHz ADCPs. The collected data are then averaged over 20  
18 min periods. Our study will focus on the tidally filtered time series of these  
19 currents. To performed the tide filtering, we used the Godin's tide filter  
20 (Godin, 1972). The cut-off period of the Godin's filter is 3.9 days.  
21  
22  
23  
24  
25  
26  
27  
28  
29  
30  
31  
32  
33  
34

35 The tidally filtered currents were projected into separate along-shore and  
36 cross-shore components. Based on the hypothesis that the current variability  
37 is strongly constrained by the topography, the along (cross) shore direction is  
38 defined by the direction which maximizes (minimizes) the current variability.  
39 Applying an Empirical Orthogonal function (EOF) method (Björnsson and  
40 Venegas, 1997) to the zonal and meridional components of the vertically  
41 averaged and tidally-filtered currents, we obtain two EOF modes on which  
42 the current variability can be projected. The eigenvector associated with the  
43 first (second) mode maximizes (minimizes) this variability and defines the  
44  
45  
46  
47  
48  
49  
50  
51  
52  
53  
54  
55  
56  
57  
58  
59  
60  
61  
62  
63  
64  
65

1  
2  
3  
4  
5  
6  
7  
8  
9  
10  
11  
12  
13  
14  
15  
16  
17  
18  
19  
20  
21  
22  
23  
24  
25  
26  
27  
28  
29  
30  
31  
32  
33  
34  
35  
36  
37  
38  
39  
40  
41  
42  
43  
44  
45  
46  
47  
48  
49  
50  
51  
52  
53  
54  
55  
56  
57  
58  
59  
60  
61  
62  
63  
64  
65

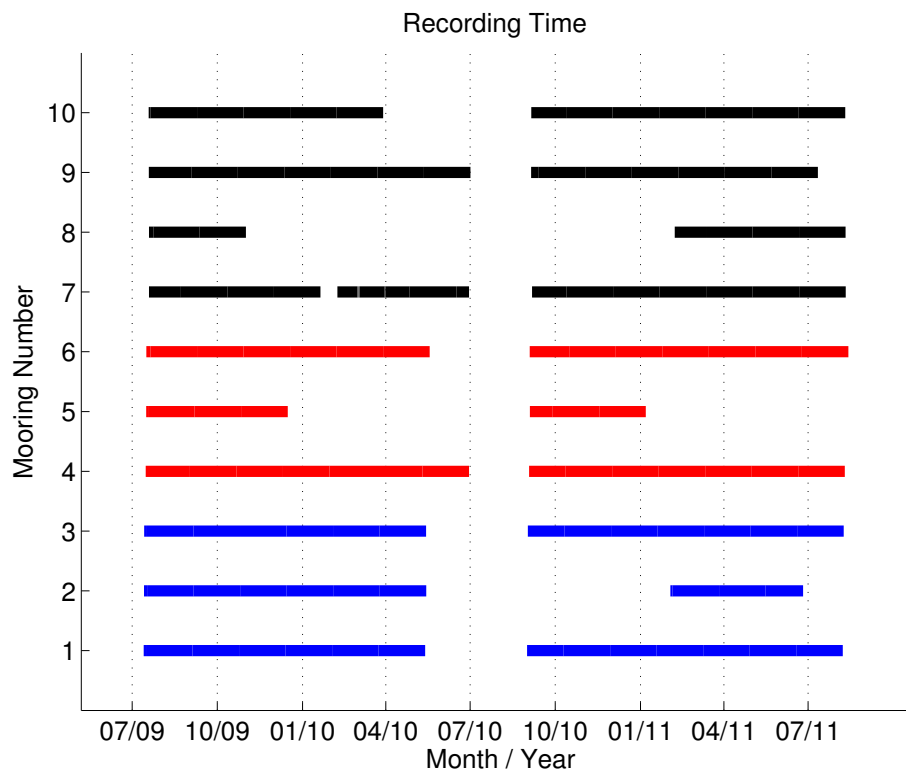


Figure 2: Length of the time record for each mooring after removing outlier data. The colors blue, red and black represent the Penmarc'h, Loire and 44°N sections



1  
2  
3  
4  
5 along (cross) shore direction. Figure 1 presents the cross-shore and along-  
6 shore directions defined by the EOF method. These directions are defined  
7 as poleward positive for the along-shore component and positive toward the  
8 coast for the cross-shore component.  
9

## 10 11 12 13 *2.2. Current processing for seasonal circulation* ★ 14

15  
16 Based on the available collected data, we process the dataset to define  
17 the seasonal currents. These currents are averaged over three month periods:  
18 January, February, March for winter; April, May, June for spring; July, Au-  
19 gust, September for summer and October, November, December for autumn.  
20 We only consider continuous time series longer than a month to define a sea-  
21 sonal time average. This month must be common to at least two moorings  
22 along each section to be taken into account. This processing allows a consis-  
23 tent analysis of the seasonal circulation along a section. Table 2 describes the  
24 seasonal time series per section for each available season. From summer 2009  
25 to summer 2011, the shortest and the longest seasonal time series are about  
26 34 days and 91 days, respectively. During the two years of measurements,  
27 the four seasons were each sampled twice. Summer 2010 is missing because  
28 during this season the instruments were retrieved and re-deployed. Thus, the  
29 associated time series are too short to be significant. Only summer 2009 and  
30 summer 2011 are analysed.  
31  
32  
33  
34  
35  
36  
37  
38  
39  
40  
41  
42  
43  
44

## 45 *2.3. ARPEGE Winds* ★ 46

47 To understand the dynamics of the BoB circulation, we compare the  
48 ASPEX data to the winds in the BoB over the two years of measurements.  
49 The winds are from the ARPEGE atmospheric general circulation model  
50  
51  
52  
53  
54  
55  
56  
57  
58  
59  
60  
61  
62  
63  
64  
65

1  
2  
3  
4  
5  
6  
7  
8  
9  
10  
11  
12  
13  
14  
15  
16  
17  
18  
19  
20  
21  
22  
23  
24  
25  
26  
27  
28  
29  
30  
31  
32  
33  
34  
35  
36  
37  
38  
39  
40  
41  
42  
43  
44  
45  
46  
47  
48  
49  
50  
51  
52  
53  
54  
55  
56  
57  
58  
59  
60  
61  
62  
63  
64  
65

		<b>Penmarch</b>	<b>Loire</b>	44°
<b>Summer 2009</b>	Start Date	07/16/2009	07/19/2009	07/22/2009
	End Date	09/30/2009	09/30/2009	09/30/2009
	Length (days)	76	73	70
	Mooring Id	1 2 3	4 5 6	7 8 9 10
<b>Autumn 2009</b>	Start Date	10/01/2009	10/01/2009	10/01/2009
	End Date	12/31/2009	12/12/2009	12/31/2009
	Length (days)	91	72	91
	Mooring Id	1 2 3	4 5 6	7 9 10
<b>Winter 2010</b>	Start Date	01/01/2010	01/01/2010	02/10/2010
	End Date	03/31/2010	03/31/2010	03/26/2010
	Length (days)	89	89	43
	Mooring Id	1 2 3	4 6	7 9 10
<b>Spring 2010</b>	Start Date	04/01/2010	04/01/2010	04/01/2010
	End Date	05/10/2010	05/15/2010	06/26/2010
	Length (days)	39	44	86
	Mooring Id	1 2 3	4 6	7 9
<b>Autumn 2010</b>	Start Date	10/01/2010	10/01/2010	10/01/2010
	End Date	12/31/2010	12/31/2010	12/31/2010
	Length (days)	91	91	91
	Mooring Id	1 3	4 5 6	7 9 10
<b>Winter 2011</b>	Start Date	02/05/2011	01/01/2011	02/09/2011
	End Date	03/31/2011	03/31/2011	03/31/2011
	Length (days)	54	89	50
	Mooring Id	1 2 3	4 6	7 8 9 10
<b>Spring 2011</b>	Start Date	04/01/2011	04/01/2011	04/01/2011
	End Date	06/22/2011	06/30/2011	06/30/2011
	Length (days)	82	90	90
	Mooring Id	1 2 3	4 6	7 8 9 10
<b>Summer 2011</b>	Start Date	07/01/2011	07/01/2011	07/01/2011
	End Date	08/04/2011	08/06/2011	08/07/2011
	Length (days)	34	36	37
	Mooring Id	1 3	4 6	7 8 10

Table 2: Seasonal Time series characteristics per season and per section. Note that there is no data for summer 2010.

1  
2  
3  
4  
5 (GCM) from Météo-France (Déqué et al., 1994). The model outputs are  
6 sampled every 6 hours and its spatial grid has a  $0.5^\circ$  resolution. We use the  
7 ARPEGE winds within a range from  $43.5^\circ\text{N}$  to  $48.5^\circ\text{N}$  and from  $1^\circ\text{W}$  to  
8  $7^\circ\text{W}$ .  
9

#### 10 11 12 13 *2.4. Time-lagged Wind-Current correlations* ★ 14

15 In section 3.5, the wind driven circulation is estimated based on the com-  
16 putation of the time-lagged correlation of the along-shore velocities with the  
17 local winds projected on axes varying on angles from 0 to  $2\pi$ . We focus on  
18 time lags shorter than 7 days in order to discuss about synoptic time scales  
19 and shorter periods. The maximum correlation and the corresponding angle  
20 allow an estimation of the wind component for which the variations of the  
21 along-shore currents and winds are in phase. We also have access to the time  
22 lags associated with these maximum values of correlation. This information  
23 is a good proxy to estimate the influence of the local winds or other forcing.  
24  
25  
26  
27  
28  
29  
30  
31  
32

### 33 34 **3. Results** ★

#### 35 36 *3.1. Wind Regimes in the Bay of Biscay* ★ 37

38 An EOF method implemented on the BoB wind field indicates that the  
39 wind field exhibits weaker spatial variation at the scale of the analysis. For  
40 the studied period, the first EOF mode explains about 77% of the total  
41 variability and the spatial structure (eigenvector) is uniform. Figure 3a shows  
42 the 1<sup>st</sup> EOF mode of the winds. It indicates that the wind variations are  
43 coherent and similar over the whole BoB.  
44  
45  
46  
47  
48  
49

50 In figure 3b, the wind vectors are spatially averaged over the domain  
51 adopted for the wind field. We present here, the seasonal evolution of this  
52  
53

1  
2  
3  
4  
5 spatial average. The winds in the BoB are expected to be southeastward in  
6  
7 the summer and mainly northeastward in the winter with transition periods  
8  
9 of two months between each phase. The transition periods should occur in  
10  
11 September/October and March/April. These changes in the wind direction  
12  
13 are called the SOMA effect (Pingree, 1999). However, the seasonal wind  
14  
15 evolution shows some inter-annual variability. The wind regime in autumn  
16  
17 2009 is strongly northeastward and they southeastward in autumn 2010.  
18  
19 This season exhibits a Navidad event Garcia-Soto and Pingree (2012). This  
20  
21 event and its influence are discussed in section 4. Furthermore, winter 2010  
22  
23 is strongly northward. This is due to two important storms that occurred  
24  
25 this winter. One of them was the Xinthia storm which caused many damages  
26  
27 in the west coast of France.

### 28 *3.2. Mean circulation*

★

29  
30  
31 The observed mean circulation (vertically and time averaged over the  
32  
33 available data) from July 2009 to August 2011 (blue arrows in figure 4)  
34  
35 is mainly poleward following the topography with currents of order of 3  
36  
37  $cm s^{-1}$ . On the slope, the mean currents tend to increase poleward while  
38  
39 the circulation on the shelf presents a less coherent spatial variability. The  
40  
41 strongest mean currents ( $\sim 5 cm s^{-1}$ ) are found at the 450 m isobath in the  
42  
43 Penmarc'h section and they decrease over the slope to  $2 cm s^{-1}$  in the Loire  
44  
45 section and in the  $44^\circ N$  section. The circulation in front of the Loire river is  
46  
47 weaker ( $1 cm s^{-1}$ ) and eastward at the 130 m isobath. In the  $44^\circ N$  section,  
48  
49 the mean current at the 60 m isobath is about  $4 cm s^{-1}$ . The results at the  
50  
51 70 m isobath in the  $44^\circ N$  section and at the 130 m isobath in front of the  
52  
53 Loire river should be analysed carefully because the associated time series

1  
2  
3  
4  
5  
6  
7  
8  
9  
10  
11  
12  
13  
14  
15  
16  
17  
18  
19  
20  
21  
22  
23  
24  
25  
26  
27  
28  
29  
30  
31  
32  
33  
34  
35  
36  
37  
38  
39  
40  
41  
42  
43  
44  
45  
46  
47  
48  
49  
50  
51  
52  
53  
54  
55  
56  
57  
58  
59  
60  
61  
62  
63  
64  
65

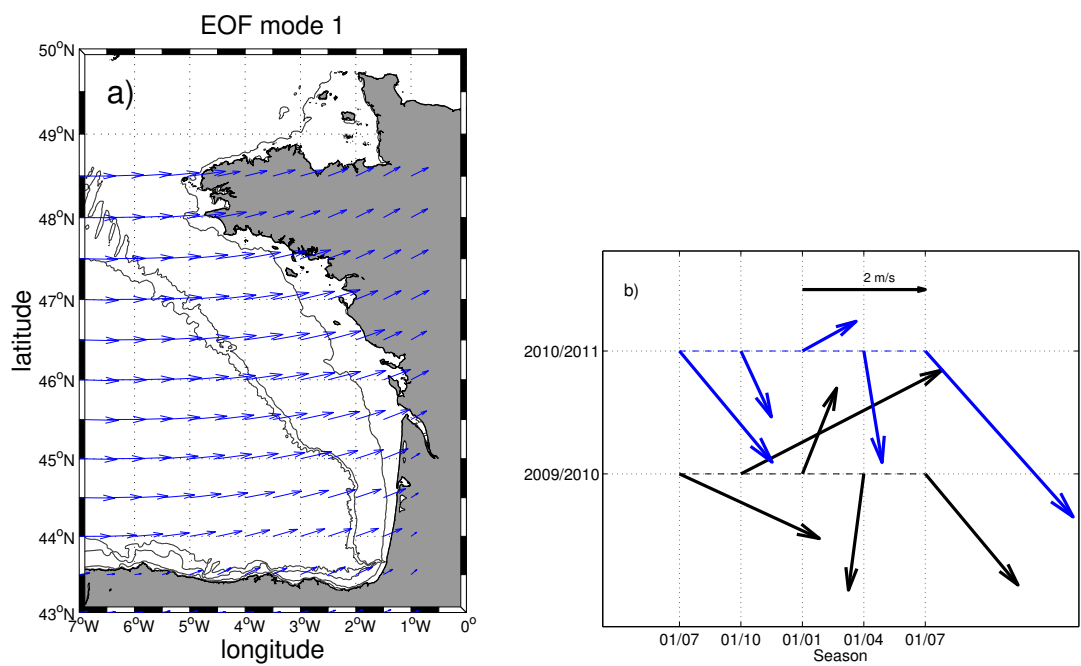


Figure 3: a) Spatial structure of the first EOF mode of the Bay of Biscay's Winds, b) Monthly averaged wind in the Bay of Biscay for the year 2009/2010 (black) and 2010/2011 (blue).

1  
2  
3  
4  
5 presents less than 200 days (thin arrows on figure 4) of data compared to  
6 more than 600 days of data for most of the others .  
7

8  
9 These mean currents are compared with the mean winds observed in the  
10 middle of each section over the two years of the experiment (red arrows).  
11 The wind at these locations presents a good proxy of the wind over the  
12 whole section. The mean winds veer southward with decreasing latitudes  
13 and the mean currents are poleward following topography. The mean winds  
14 are eastward with an intensity of  $2m s^{-1}$  along the Penmarc'h latitude and  
15 turn southward in the southern part of the BoB. Winds are opposed to the  
16 currents in most locations.  
17  
18  
19  
20  
21  
22  
23

### 24 *3.3. Seasonal circulation* ★

#### 25 *3.3.1. Depth-averaged circulation* ★

26  
27 The depth averaged seasonal circulation is represented on Figure 5a. Like  
28 the mean circulation over the two years, seasonal currents are generally pole-  
29 ward and they flow along the topography.  
30  
31  
32  
33

34 In autumn, the circulation is poleward over all the BoBSS. Differences  
35 appear in the intensity of the circulation. The intensity of the circulation in  
36 the northern part of the BoBSS (Penmarc'h and Loire sections) is similar for  
37 currents at the 60 and 450 m isobaths of about  $5 cm s^{-1}$  and weaker currents  
38 of about  $2 cm s^{-1}$  at the 130 m isobath. In the  $44^{\circ}N$  section the weaker ( $2$   
39  $cm s^{-1}$ ) currents are near the coast (60 m isobath). The currents increase  
40 off shore with an intensity of about  $5 cm s^{-1}$ .  
41  
42  
43  
44  
45  
46  
47  
48  
49

50 In winter, the currents are poleward along the 60 m isobath increasing  
51 northward with a maximum at Penmarc'h about  $5 cm s^{-1}$ . Along the 130  
52  
53

1  
2  
3  
4  
5  
6  
7  
8  
9  
10  
11  
12  
13  
14  
15  
16  
17  
18  
19  
20  
21  
22  
23  
24  
25  
26  
27  
28  
29  
30  
31  
32  
33  
34  
35  
36  
37  
38  
39  
40  
41  
42  
43  
44  
45  
46  
47  
48  
49  
50  
51  
52  
53  
54  
55  
56  
57  
58  
59  
60  
61  
62  
63  
64  
65

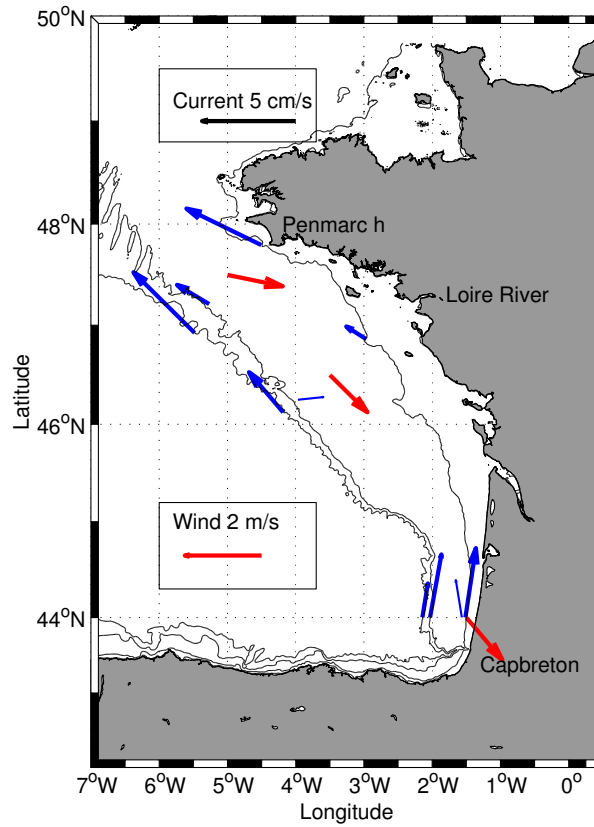


Figure 4: Two years average of the vertically averaged currents (blue arrows) and mean winds (red arrows) for the two years of the experiment. The black lines are the 60, 130 and 450 m isobaths. The thin arrows indicate data coverage less than 200 days of data

1  
2  
3  
4  
5 m isobath, the winter currents are poleward and about  $3 \text{ cm s}^{-1}$  in the  
6 Penmarc'h and  $44^\circ\text{N}$  sections. The circulation on the upper slope (450 m  
7 isobath) in winter is also poleward increasing southward with a maximum in  
8 the  $44^\circ\text{N}$  section about  $5 \text{ cm s}^{-1}$ .  
9

10  
11  
12  
13  
14 In spring, the currents are weakly poleward almost everywhere ( $\sim 1 \text{ cm}$   
15  $\text{s}^{-1}$ ) in the BoBSS. However, two moorings present different behaviors. The  
16 spring currents in the Penmarc'h section on the upper part of the slope (450  
17 m isobath ) are strong ( $5 \text{ cm s}^{-1}$ ) and the currents at the 60 m isobath in the  
18 Loire river section are slightly southward in the same direction as the mean  
19 winds over all the area for spring.  
20  
21  
22  
23  
24  
25  
26

27  
28 The summer circulation is globally weaker than during winter and au-  
29 tumn. The currents in the Penmarc'h section are poleward with a maximum  
30 at the 60 m isobath ( $5 \text{ cm s}^{-1}$ ) and a minimum at the 130 m isobath ( $\sim 1$   
31  $\text{cm s}^{-1}$ ). In the Loire section, the currents are eastward on the shelf (60 and  
32 130 m isobaths ) and poleward on the upper slope (450 m isobath ). In the  
33  $44^\circ\text{N}$  section, the currents near the coast (60 m isobath ) are poleward and  
34 the strongest in the area ( $5 \text{ cm s}^{-1}$ ). At the 130 and 450 m isobaths , the  
35 currents of the  $44^\circ\text{N}$  section are equatorward with an amplitude of  $\sim 1 \text{ cm}$   
36  $\text{s}^{-1}$ .  
37  
38  
39  
40  
41  
42  
43  
44  
45  
46

47 The seasonal variance of the tidally-filtered depth averaged currents is  
48 presented in Figure 5b. Similar to the seasonal averages, the current vari-  
49 ability is constrained by the topography with larger variances close to the  
50  
51  
52  
53  
54  
55  
56  
57  
58  
59  
60  
61  
62  
63  
64  
65



1  
2  
3  
4  
5  
6  
7  
8  
9  
10  
11  
12  
13  
14  
15  
16  
17  
18  
19  
20  
21  
22  
23  
24  
25  
26  
27  
28  
29  
30  
31  
32  
33  
34  
35  
36  
37  
38  
39  
40  
41  
42  
43  
44  
45  
46  
47  
48  
49  
50  
51  
52  
53  
54  
55  
56  
57  
58  
59  
60  
61  
62  
63  
64  
65

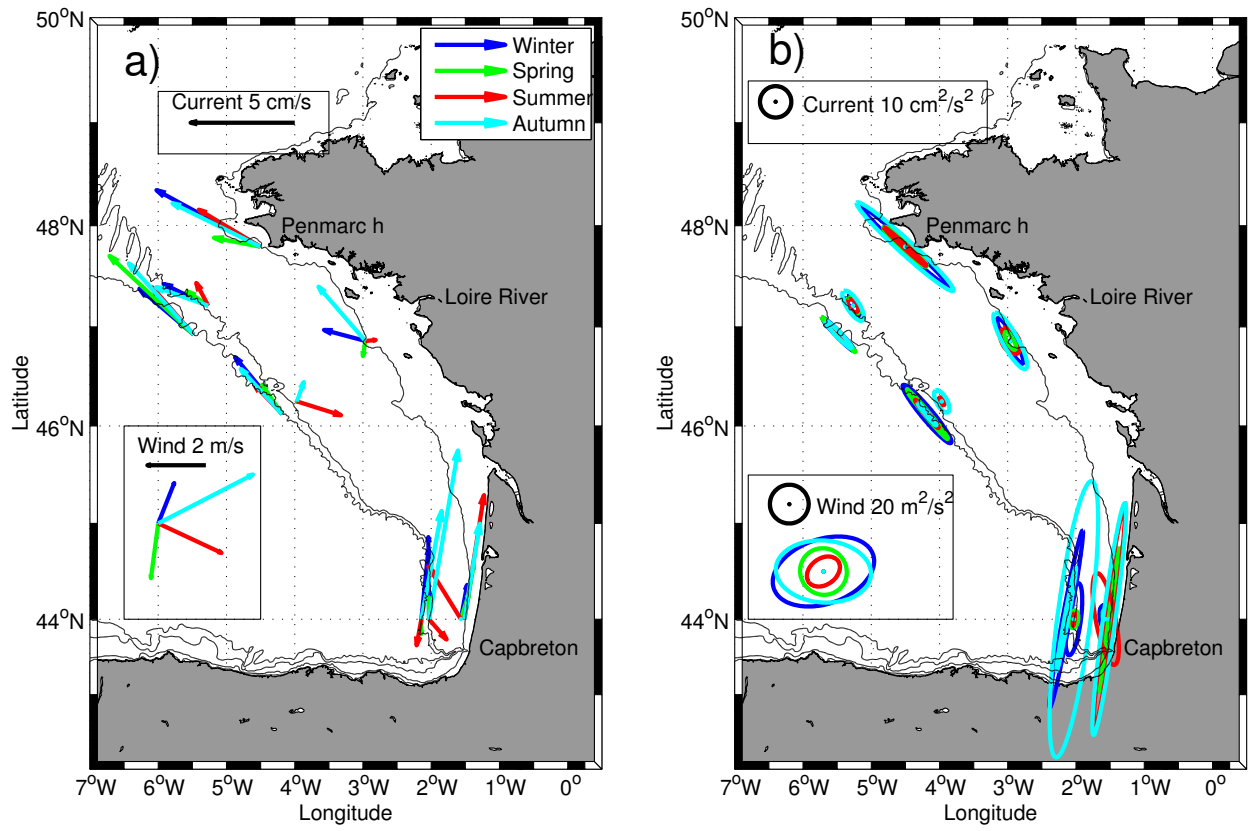


Figure 5: a) Seasonal average of depth averaged currents. Between 45 °N-6 °W, seasonal and spatial average of the winds over the domain. Summer season at all locations and spring in the Penmarc'h section present time series of about a month in one of the two sampled seasons. b) Seasonal variability of the depth averaged currents. At 45 °N-6 °W, seasonal variability of the averaged winds over the domain. Black lines indicates the 60, 130 and 450 m isobaths

1  
2  
3  
4  
5 coast and on the upper slope. The variance in autumn is the strongest along  
6 all sections except in the Loire section on the upper slope (isobath 450 m)  
7 where the variance reaches its smallest value in autumn ( $10 \text{ cm}^2 \text{ s}^{-2}$ ). Cur-  
8 rent variance amplitude during this season ranges from  $6 \text{ cm}^2 \text{ s}^{-2}$  over the  
9 130 m isobath in the Loire section to  $100 \text{ cm}^2 \text{ s}^{-2}$  in the  $44^\circ\text{N}$  section over  
10 the same isobath. In winter, the current variances remain intense with values  
11 around  $63 \text{ cm}^2 \text{ s}^{-2}$  on the upper slope in the  $44^\circ\text{N}$  section or  $40 \text{ cm}^2 \text{ s}^{-2}$   
12 above the 60 m isobath in the Penmarc'h section. In spring and summer,  
13 current variances are weaker. For example, over the 130 m isobath in the  
14 Penmarc'h and  $44^\circ\text{N}$  sections, variance falls to  $6 \text{ cm}^2 \text{ s}^{-2}$ .  
15  
16  
17  
18  
19  
20  
21  
22  
23  
24

### 25 *3.3.2. Seasonal vertical current profiles*

★

26  
27 Figure 6 presents the seasonal vertical profiles of the along-shore and  
28 cross-shore current components for each section. These profiles allow to  
29 highlight the different features between the shelf and the slope circulations.  
30  
31  
32

#### 33 *Over the 450 m isobath.*

34  
35 On the upper slope (450 m isobath), vertical profiles of the along-shore cur-  
36 rent exhibit a poleward circulation except in spring and summer along the  
37  $44^\circ\text{N}$  section. However, the vertical structure exhibits a spatial and temporal  
38 variability. In winter, Loire and  $44^\circ\text{N}$  sections have an increasing velocity  
39 from near bottom depth (almost null velocity) to surface (reaching  $10 \text{ cm}$   
40  $\text{s}^{-1}$ ). In autumn and summer along the Penmarc'h and Loire sections, the  
41 profile have a maximum speed at around 130 m depth ( $\sim 8 \text{ cm s}^{-1}$ ). We  
42 observe three groups of profiles:  
43  
44  
45  
46  
47  
48  
49

50 - linearly increasing speed from depth to surface observed during in autumn  
51  
52  
53  
54  
55  
56  
57  
58  
59  
60  
61  
62  
63  
64  
65

1  
2  
3  
4  
5  
6  
7  
8  
9  
10  
11  
12  
13  
14  
15  
16  
17  
18  
19  
20  
21  
22  
23  
24  
25  
26  
27  
28  
29  
30  
31  
32  
33  
34  
35  
36  
37  
38  
39  
40  
41  
42  
43  
44  
45  
46  
47  
48  
49  
50  
51  
52  
53  
54  
55  
56  
57  
58  
59  
60  
61  
62  
63  
64  
65

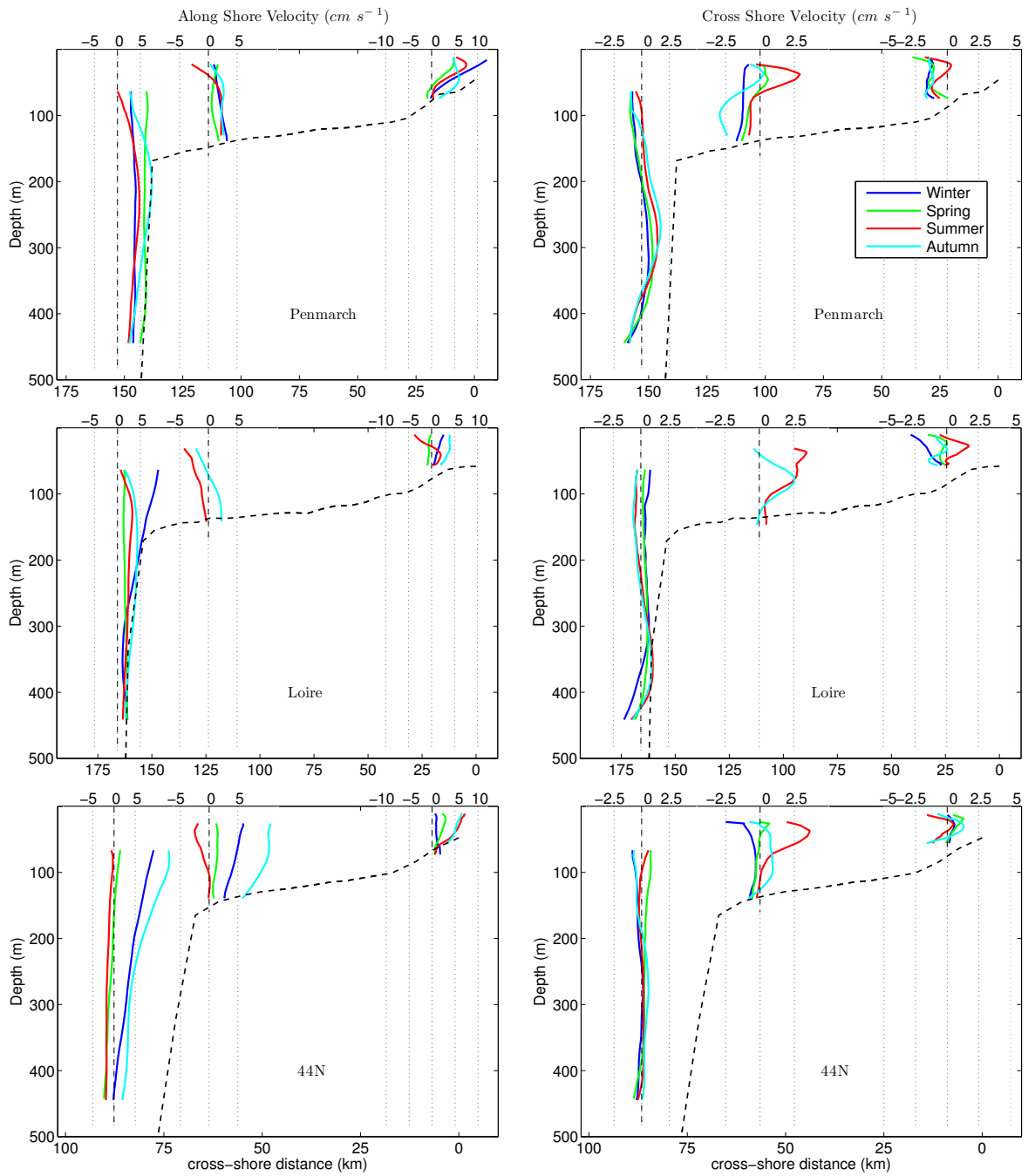


Figure 6: Seasonal vertical profiles of the along-shore (left panels) positive poleward and cross-shore (right panels) positive shoreward components of the currents for Penmarc'h (upper panels), Loire (mid panels) and 44°N (bottom panels) sections. Blue lines: winter, Green lines: spring, Red lines: summer and Cyan lines: autumn. X-axis scales of the vertical profile are in  $cm s^{-1}$  and changes for each isobath. On all these graphs, the position of the profiles have been adjusted for the sake of clarity.

1  
2  
3  
4  
5 and winter in the southern part of the BoBSS,  
6  
7 - profiles with a maximum poleward speed around 130 m depth in spring and  
8  
9 summer in the northern part of the BoBSS,  
10  
11 - profiles with equatorward deep velocities and weak currents at surface in  
12  
13 spring and summer in the South of the BoBSS.  
14  
15

16 The vertical profiles of the cross-shore currents are characterized by weaker  
17  
18 velocities than in the along-shore direction. The maximum observed cross-  
19  
20 shore seasonal mean velocity is  $\sim 2 \text{ cm s}^{-1}$  in the Penmarc'h section in au-  
21  
22 tumn. We observe downslope velocities near the bottom and upslope veloc-  
23  
24 ities above 350-400 meter depth with a maximum at 250-350 meter depth.  
25  
26 The depth of the current inversion slightly changes with the season. Along  
27  
28 the  $44^\circ\text{N}$  section, the seasonal velocities are weak ( $1 \text{ cm s}^{-1}$ ) and shows no  
29  
30 important vertical shear and no important seasonal variability.  
31

32 *Over the 130 m isobath.*  
33

34 From autumn to spring, currents flow mainly poleward except in a surface  
35  
36 layer along Loire section (above 70 m depth). However, the shape of profiles  
37  
38 differs between  $44^\circ\text{N}$  and Penmarc'h sections. Indeed, largest velocities are  
39  
40 observed near the surface in the south and near the bottom in the north  
41  
42 ( $\sim 4 \text{ cm s}^{-1}$ ). Another difference between these two sections is that the  
43  
44 seasonal variability is strong along the  $44^\circ\text{N}$  section with maximum speeds  
45  
46 in autumn reaching  $> 10 \text{ cm s}^{-1}$ . The summer remains the only season when  
47  
48 equatorward currents are measured (3 to  $5 \text{ cm s}^{-1}$  at surface).  
49

50 Along this isobath, cross-shore currents have amplitudes slightly less than  
51  
52 the along-shore current amplitude. In summer, significant upslope currents  
53  
54

1  
2  
3  
4  
5 ( $\sim 2.5 \text{ cm s}^{-1}$ ) are observed. The vertical shear, characterized by a sub-  
6 surface onshore velocity maximum, is also strong along the Penmarc'h and  
7 Loire sections and in summer along the  $44^\circ\text{N}$  section. On the contrary, in  
8 winter, profiles are more vertical and offshore.  
9

10  
11  
12  
13 *Over the 60 m isobath.*

14  
15 Along the 60 m isobath, the along-shore currents are mainly poleward reach-  
16 ing  $12 \text{ cm s}^{-1}$  in the Penmarc'h section in winter at the surface. The mean  
17 along-shore velocities are almost null at the bottom and increase toward the  
18 surface. Only the summer profile for the Loire section differs from surface  
19 equatorward currents with an intensity of  $5 \text{ cm s}^{-1}$ .  
20  
21

22 The vertical profiles of the cross-shore currents at the 60 m isobath are  
23 coherent with profiles for the 130 m isobath showing a subsurface maximum  
24 trend during spring, summer and autumn. In winter, the vertical profile  
25 shape is different. Vertical velocity gradients are weaker suggesting the im-  
26 portance of seasonal stratification for the rest of the year.  
27  
28  
29  
30  
31  
32  
33

### 34 35 3.4. Weekly circulation

36  
37  
38 The amount of energy represented by the variance ellipses and their vari-  
39 ability depicted in the previous section (figure 5) led us to observe the results  
40 at higher frequencies. The tidally filtered time series of the weekly circulation  
41 in the BoBSS at near surface and near bottom depths is presented in figure  
42 7. The weekly averages of the along-shore currents along the 60, 130 and 450  
43 m isobaths show strong along-shore currents values reaching  $30 \text{ cm s}^{-1}$  close  
44 to the surface at all isobaths. The results for the 130 m isobath are not pre-  
45 sented because they are similar to the times series at the 450 m isobath with  
46  
47  
48  
49  
50  
51  
52  
53  
54  
55  
56  
57  
58  
59  
60  
61  
62  
63  
64  
65

\*

1  
2  
3  
4  
5 strong currents that occurred for autumn at the south of BoBSS (figure 5).  
6  
7 Furthermore, at this isobath, the circulation for the two sections (Penmarc'h  
8 and Loire) present some gaps in the time series. In the 44 °N section, the 450  
9 m isobath present the strongest along-shore currents. In autumn 2009 and  
10 autumn 2010, the current intensity reaches  $> 30 \text{ cm s}^{-1}$ . These seasonal  
11 two events are marked by several monthly episodes of intensified poleward  
12 currents. The near bottom cross-shore currents at this location are always  
13 downslope and increase during strong poleward currents (not shown). The  
14 strongest currents ( $> 20 \text{ cm s}^{-1}$ ) along 60 m isobath are at Penmarc'h in  
15 spring 2010 and 2011 and in the 44 °N section in autumn 2009 and 2010.  
16 At the Penmarc'h section, the currents are surface intensified and at the the  
17 44 °N section the strong currents are also observed near the bottom. These  
18 strong current events occurring in the 44 °N section, either at the 60 m iso-  
19 bath or the 450 m isobath (Blue lines), are followed by a current peak in the  
20 Loire section (Black lines). They occurred in autumn (6<sup>th</sup> November 2009 at  
21 the 60 m isobath and  $\sim 15^{\text{th}}$  November 2010 at the 450 m isobath) or early  
22 winter ( $\sim 1^{\text{st}}$  January 2011 at the 450 m isobath).  
23  
24  
25  
26  
27  
28  
29  
30  
31  
32  
33  
34  
35  
36

37 The summer and autumn 2009 near bottom circulation recorded at the  
38 44 °N section at the 60 m isobath is not correlated with the one at the Pen-  
39 marc'h section. After the barotropic events occurring at the 44 °N section,  
40 figure 7 shows some coherent variations of about  $10 \text{ cm s}^{-1}$  for the three  
41 sections from January to May 2010 with a period of about a month along  
42 the 60 m isobath. These coherent oscillations seem to cease at the beginning  
43 of summer seasons. This specific behaviour also occurs after autumn 2010  
44 and during winter 2011. At the 450 m isobath , the near bottom circulation  
45  
46  
47  
48  
49  
50  
51  
52  
53  
54  
55  
56  
57  
58  
59  
60  
61  
62  
63  
64  
65

1  
2  
3  
4  
5  
6  
7  
8  
9  
10  
11  
12  
13  
14  
15  
16  
17  
18  
19  
20  
21  
22  
23  
24  
25  
26  
27  
28  
29  
30  
31  
32  
33  
34  
35  
36  
37  
38  
39  
40  
41  
42  
43  
44  
45  
46  
47  
48  
49  
50  
51  
52  
53  
54  
55  
56  
57  
58  
59  
60  
61  
62  
63  
64  
65

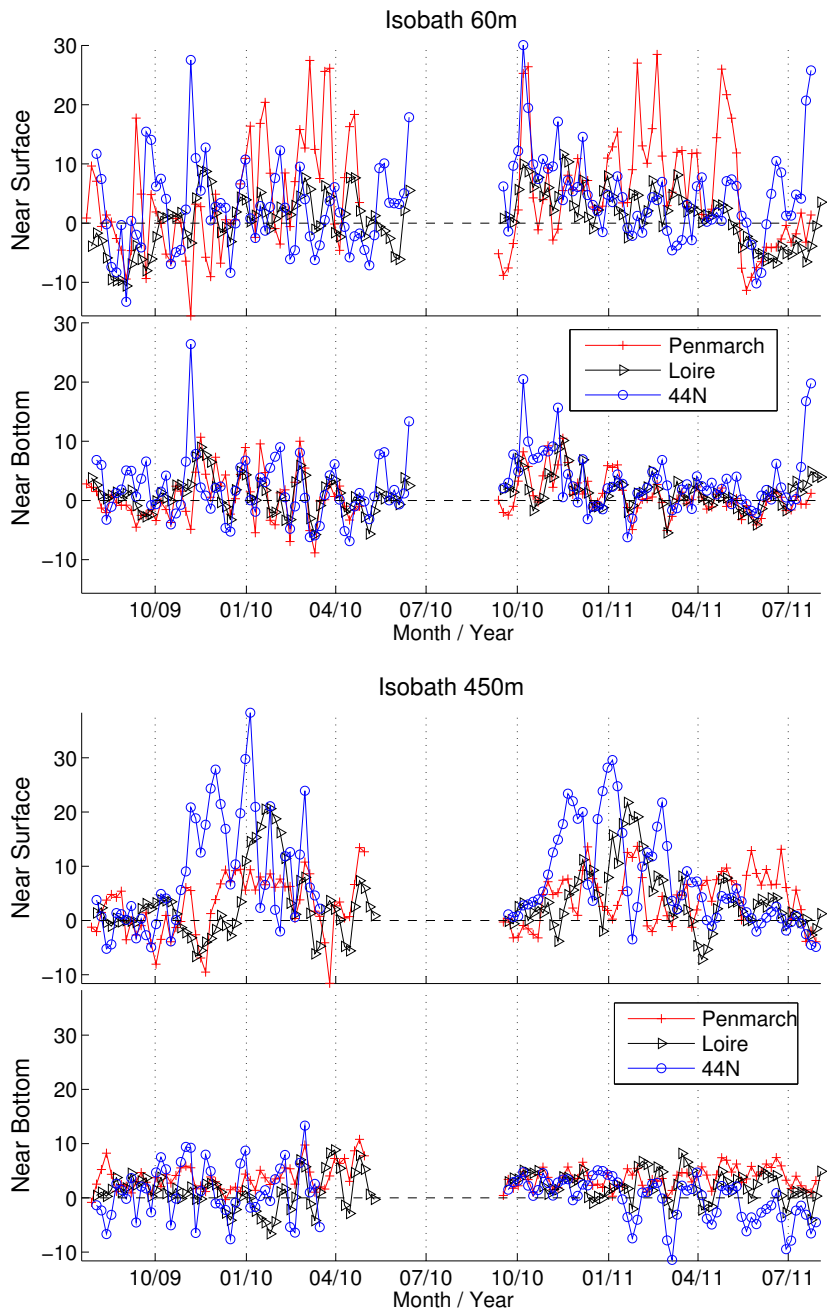


Figure 7: Weekly average of the along-shore velocities in  $cm\ s^{-1}$  near the bottom depth and near the surface. Upper and lower panels present the velocities at the 60 m isobath (surface: 7 m depth and bottom: 53 m depth) and 450 m (surface: 53 m depth and bottom: 378 m depth), respectively. Red, Black and Blue lines are velocities at moorings along Penmarch, Loire and 44°N sections respectively.

1  
2  
3  
4  
5 also shows behaviour changes according to the seasons. The near bottom  
6 currents are in the range of  $\pm 5 \text{ cm s}^{-1}$  for summer and autumn of both  
7 years (2009 and 2010) while they stay in the range of  $\pm 10 \text{ cm s}^{-1}$  for the  
8 rest of the year (winter and spring). Oscillations observed near the bottom  
9 such as the ones observed on the 60 m isobath occurred only in the south of  
10 the BoB for late autumn 2009, winter 2010, winter and spring 2011. In the  
11 Penmarc'h and Loire sections the variability of the along-shore current along  
12 the 450 m isobath stands within a range of  $-1 \text{ cm s}^{-1}$  to  $10 \text{ cm s}^{-1}$ . The  
13 450 m isobath circulations in these sections for stratified seasons (summer  
14 and autumn) occurs in the same period of time while for winter and spring,  
15 the Loire section currents follow the  $44^\circ\text{N}$  section current variations.  
16  
17

18  
19  
20  
21  
22  
23  
24  
25  
26 Coherent flows all over the BoB or over a large part of the area may be  
27 the response to large scale forcing. In the section 4, we discuss the possibility  
28 that large scale forcing leads to the circulation in the BoB.  
29  
30

### 31 32 33 *3.5. Wind Driven Circulation* ★

34  
35 A first step toward the understanding of the tidally filtered BoB circula-  
36 tion is to estimate the wind driven circulation part from the total circulation.  
37 Figure 8 presents the maximum values of the time lagged correlations of the  
38 depth averaged along-shore velocities and the local along-shore winds stress  
39 along the 60 m isobath. This analysis focus on the seasonal behaviour of the  
40 correlations of the wind stress with the depth averaged along-shore currents.  
41 The correlations are presented as a function of the direction of the wind com-  
42 ponent which lead to these values. They stand within a range of  $\sim 0.4-0.8$ .  
43  
44  
45  
46  
47  
48  
49  
50  
51  
52  
53  
54  
55  
56  
57  
58  
59  
60  
61  
62  
63  
64  
65  
66  
67  
68  
69  
70  
71  
72  
73  
74  
75  
76  
77  
78  
79  
80  
81  
82  
83  
84  
85  
86  
87  
88  
89  
90  
91  
92  
93  
94  
95  
96  
97  
98  
99  
100  
101  
102  
103  
104  
105  
106  
107  
108  
109  
110  
111  
112  
113  
114  
115  
116  
117  
118  
119  
120  
121  
122  
123  
124  
125  
126  
127  
128  
129  
130  
131  
132  
133  
134  
135  
136  
137  
138  
139  
140  
141  
142  
143  
144  
145  
146  
147  
148  
149  
150  
151  
152  
153  
154  
155  
156  
157  
158  
159  
160  
161  
162  
163  
164  
165  
166  
167  
168  
169  
170  
171  
172  
173  
174  
175  
176  
177  
178  
179  
180  
181  
182  
183  
184  
185  
186  
187  
188  
189  
190  
191  
192  
193  
194  
195  
196  
197  
198  
199  
200  
201  
202  
203  
204  
205  
206  
207  
208  
209  
210  
211  
212  
213  
214  
215  
216  
217  
218  
219  
220  
221  
222  
223  
224  
225  
226  
227  
228  
229  
230  
231  
232  
233  
234  
235  
236  
237  
238  
239  
240  
241  
242  
243  
244  
245  
246  
247  
248  
249  
250  
251  
252  
253  
254  
255  
256  
257  
258  
259  
260  
261  
262  
263  
264  
265  
266  
267  
268  
269  
270  
271  
272  
273  
274  
275  
276  
277  
278  
279  
280  
281  
282  
283  
284  
285  
286  
287  
288  
289  
290  
291  
292  
293  
294  
295  
296  
297  
298  
299  
300  
301  
302  
303  
304  
305  
306  
307  
308  
309  
310  
311  
312  
313  
314  
315  
316  
317  
318  
319  
320  
321  
322  
323  
324  
325  
326  
327  
328  
329  
330  
331  
332  
333  
334  
335  
336  
337  
338  
339  
340  
341  
342  
343  
344  
345  
346  
347  
348  
349  
350  
351  
352  
353  
354  
355  
356  
357  
358  
359  
360  
361  
362  
363  
364  
365  
366  
367  
368  
369  
370  
371  
372  
373  
374  
375  
376  
377  
378  
379  
380  
381  
382  
383  
384  
385  
386  
387  
388  
389  
390  
391  
392  
393  
394  
395  
396  
397  
398  
399  
400  
401  
402  
403  
404  
405  
406  
407  
408  
409  
410  
411  
412  
413  
414  
415  
416  
417  
418  
419  
420  
421  
422  
423  
424  
425  
426  
427  
428  
429  
430  
431  
432  
433  
434  
435  
436  
437  
438  
439  
440  
441  
442  
443  
444  
445  
446  
447  
448  
449  
450  
451  
452  
453  
454  
455  
456  
457  
458  
459  
460  
461  
462  
463  
464  
465  
466  
467  
468  
469  
470  
471  
472  
473  
474  
475  
476  
477  
478  
479  
480  
481  
482  
483  
484  
485  
486  
487  
488  
489  
490  
491  
492  
493  
494  
495  
496  
497  
498  
499  
500  
501  
502  
503  
504  
505  
506  
507  
508  
509  
510  
511  
512  
513  
514  
515  
516  
517  
518  
519  
520  
521  
522  
523  
524  
525  
526  
527  
528  
529  
530  
531  
532  
533  
534  
535  
536  
537  
538  
539  
540  
541  
542  
543  
544  
545  
546  
547  
548  
549  
550  
551  
552  
553  
554  
555  
556  
557  
558  
559  
560  
561  
562  
563  
564  
565  
566  
567  
568  
569  
570  
571  
572  
573  
574  
575  
576  
577  
578  
579  
580  
581  
582  
583  
584  
585  
586  
587  
588  
589  
590  
591  
592  
593  
594  
595  
596  
597  
598  
599  
600  
601  
602  
603  
604  
605  
606  
607  
608  
609  
610  
611  
612  
613  
614  
615  
616  
617  
618  
619  
620  
621  
622  
623  
624  
625  
626  
627  
628  
629  
630  
631  
632  
633  
634  
635  
636  
637  
638  
639  
640  
641  
642  
643  
644  
645  
646  
647  
648  
649  
650  
651  
652  
653  
654  
655  
656  
657  
658  
659  
660  
661  
662  
663  
664  
665  
666  
667  
668  
669  
670  
671  
672  
673  
674  
675  
676  
677  
678  
679  
680  
681  
682  
683  
684  
685  
686  
687  
688  
689  
690  
691  
692  
693  
694  
695  
696  
697  
698  
699  
700  
701  
702  
703  
704  
705  
706  
707  
708  
709  
710  
711  
712  
713  
714  
715  
716  
717  
718  
719  
720  
721  
722  
723  
724  
725  
726  
727  
728  
729  
730  
731  
732  
733  
734  
735  
736  
737  
738  
739  
740  
741  
742  
743  
744  
745  
746  
747  
748  
749  
750  
751  
752  
753  
754  
755  
756  
757  
758  
759  
760  
761  
762  
763  
764  
765  
766  
767  
768  
769  
770  
771  
772  
773  
774  
775  
776  
777  
778  
779  
780  
781  
782  
783  
784  
785  
786  
787  
788  
789  
790  
791  
792  
793  
794  
795  
796  
797  
798  
799  
800  
801  
802  
803  
804  
805  
806  
807  
808  
809  
810  
811  
812  
813  
814  
815  
816  
817  
818  
819  
820  
821  
822  
823  
824  
825  
826  
827  
828  
829  
830  
831  
832  
833  
834  
835  
836  
837  
838  
839  
840  
841  
842  
843  
844  
845  
846  
847  
848  
849  
850  
851  
852  
853  
854  
855  
856  
857  
858  
859  
860  
861  
862  
863  
864  
865  
866  
867  
868  
869  
870  
871  
872  
873  
874  
875  
876  
877  
878  
879  
880  
881  
882  
883  
884  
885  
886  
887  
888  
889  
890  
891  
892  
893  
894  
895  
896  
897  
898  
899  
900  
901  
902  
903  
904  
905  
906  
907  
908  
909  
910  
911  
912  
913  
914  
915  
916  
917  
918  
919  
920  
921  
922  
923  
924  
925  
926  
927  
928  
929  
930  
931  
932  
933  
934  
935  
936  
937  
938  
939  
940  
941  
942  
943  
944  
945  
946  
947  
948  
949  
950  
951  
952  
953  
954  
955  
956  
957  
958  
959  
960  
961  
962  
963  
964  
965  
966  
967  
968  
969  
970  
971  
972  
973  
974  
975  
976  
977  
978  
979  
980  
981  
982  
983  
984  
985  
986  
987  
988  
989  
990  
991  
992  
993  
994  
995  
996  
997  
998  
999  
1000



1  
2  
3  
4  
5 The correlations at the 60 m isobath can be split into two groups. Some  
6 points are localized close to the along-shore directions showing that wind in  
7 the along-shore direction has maximum effect and the other group of points  
8 is localized to the west of these along-shore directions. We see that these two  
9 groups may be better characterized as a geographical criterion rather than  
10 a seasonal influence. Indeed, the depth-averaged along-shore currents in the  
11 Penmarc'h and Loire sections are correlated with winds projected on the lo-  
12 cal along-shore directions while in the 44 °N section the along shore currents  
13 are well correlated with westerlies. In the Loire section, the highest correla-  
14 tion occurs in spring while autumn winds are well correlated with the depth  
15 averaged circulation in the Penmarc'h section. In both sections, correlations  
16 slightly decrease in summer. In the 44 °N section, only the correlation in win-  
17 ter 2010 (blue triangles) is aligned with the local along-shore direction (i.e:  
18 north-south). All other seasonal along-shore current / wind correlations at  
19 this section are not aligned with the along-shore direction and the associated  
20 points are part of the second group of points that we have define. Some other  
21 correlation points are not aligned with the local topography in the Penmarc'h  
22 section for winter 2010 and Loire section for summer 2009, winter 2010 and  
23 autumn 2010. Thus, the correlations are not influenced by the local winds  
24 and might be indicative of remote forcing mechanism transmitted by coastal  
25 trapped waves.  
26  
27  
28  
29  
30  
31  
32  
33  
34  
35  
36  
37  
38  
39  
40  
41  
42  
43  
44

45 Figure 9 presents the time lags in days which gives the maximum corre-  
46 lations presented in the figure 8. The maximum correlation is obtained for  
47 different time lags from 0 to 3.5 days. The Penmarc'h and Loire sections  
48 present either time lags of  $\sim 10$  hours or longer time lags from 2.5 to 3.5  
49  
50  
51  
52  
53  
54  
55  
56  
57  
58  
59  
60  
61  
62  
63  
64  
65

1  
2  
3  
4  
5  
6  
7  
8  
9  
10  
11  
12  
13  
14  
15  
16  
17  
18  
19  
20  
21  
22  
23  
24  
25  
26  
27  
28  
29  
30  
31  
32  
33  
34  
35  
36  
37  
38  
39  
40  
41  
42  
43  
44  
45  
46  
47  
48  
49  
50  
51  
52  
53  
54  
55  
56  
57  
58  
59  
60  
61  
62  
63  
64  
65

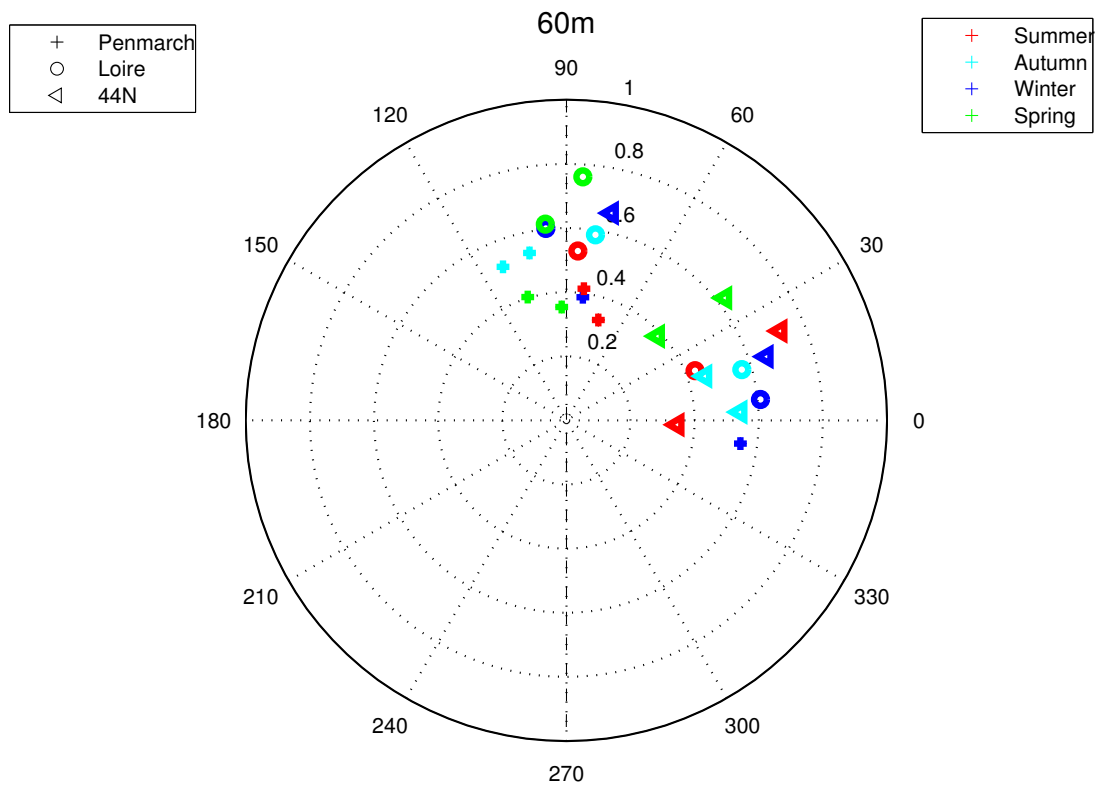


Figure 8: Maximum correlations of the depth averaged along-shore velocities at the 60 m isobath with the local wind. The radii give the value of the correlation, the azimuths give the wind orientation relative to the poleward along-shore circulation where the maximum correlation is reached. The crosses, circles and triangles are the Penmarch, Loire and 44°N section's moorings, respectively. The red, cyan, blue and green symbols represent the summer, autumn, winter and spring seasons, respectively. The black dashed lines represents the local along-shore direction of the 60 m isobath at Penmarch, Loire and 44°N sections.

1  
2  
3  
4  
5  
6  
7  
8  
9  
10  
11  
12  
13  
14  
15  
16  
17  
18  
19  
20  
21  
22  
23  
24  
25  
26  
27  
28  
29  
30  
31  
32  
33  
34  
35  
36  
37  
38  
39  
40  
41  
42  
43  
44  
45  
46  
47  
48  
49  
50  
51  
52  
53  
54  
55  
56  
57  
58  
59  
60  
61  
62  
63  
64  
65

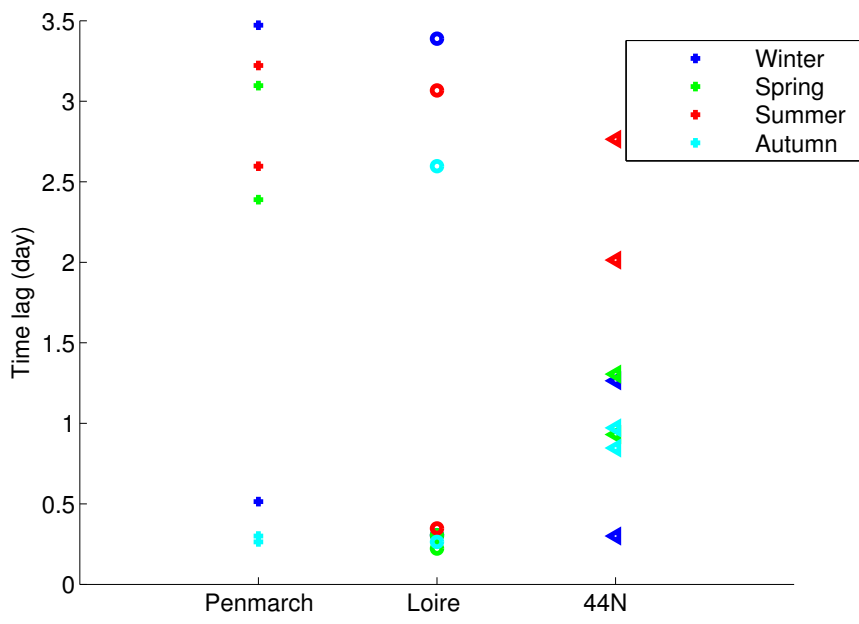


Figure 9: Time lags in days which gives the maximum correlation values presented in the figure 8. The time lags are presented per section and per season: winter in blue, spring in green, summer in red and autumn in cyan.

1  
2  
3  
4  
5  
6  
7  
8  
9  
10  
11  
12  
13  
14  
15  
16  
17  
18  
19  
20  
21  
22  
23  
24  
25  
26  
27  
28  
29  
30  
31  
32  
33  
34  
35  
36  
37  
38  
39  
40  
41  
42  
43  
44  
45  
46  
47  
48  
49  
50  
51  
52  
53  
54  
55  
56  
57  
58  
59  
60  
61  
62  
63  
64  
65

days. In the 44°N section, the time lags are about 1 day. In the summer season, the time lags increase to 2-3 days and only winter 2010 have time lag of 10 hours. Most of the correlation points aligned with the local along-shore direction have shorter times lags of 10 hours.

## 4. Discussion ★

### 4.1. Bay of Biscay Circulation ★

#### 4.1.1. Mean Circulation ★

The area is characterized by a mean wind veering from eastward to south-eastward following the edge of the Azores anticyclone (figure 4) (Isemer and Hasse, 1987). Through the Ekman transport, the mean wind regime would tend to drive a southward to southwestward flow. However, the tidally-filtered circulation upon the BoBSS is characterized by a mean poleward current. It is interesting to compare the circulation in the BoB to the one over the Mid Atlantic Bight (MAB) for several reasons. Their geometry are both complex with presence of canyons and promontories, they are both located at mid-latitudes, the tide currents are comparable, their stratification are both influenced by freshwater run off and summer heat fluxes. Furthermore, over the MAB, the winds are also perpendicular to the coast (Lentz, 2008) and the mean flow is oriented in the direction leaving the shallow water on the right. Different forcing mechanisms of the mean circulation have been proposed. On one hand, the runoff of freshwater from the river, upwelling dynamics or frontogenesis can force a cross shelf density gradient which contributes to force an along-shore current (Csanady, 1978; Beardsley and Winant, 1979). On the other hand, the shelf circulation is viewed as a

1  
2  
3  
4  
5 boundary layer of the open ocean, thus, indirectly driven by the large scale  
6 wind stress and heat fluxes which leads to an along-shore pressure gradient  
7 (Csanady, 1978). This study indicate that the shelf circulation is most likely  
8 a response to the boundary conditions provided by the open ocean and from  
9 the coastal circulation that occurs north to the MAB (Chapman and Beard-  
10 sley, 1989). However Lentz (2008) recently showed that the buoyancy driven  
11 flow in equilibrium with the cross shelf density gradient can be described by  
12 observations after simply removing the wind driven circulation. Thus, the  
13 shelf and upper slope tidally-filtered circulation could be the combination of  
14 large scale and local forcing. This likely simultaneous influence of different  
15 forcing scales brings the complexity of studying shelf and slope circulations.  
16 Our study suggests such complexity by observing two different dynamics on  
17 the upper slope and the shelf (figure 7) but the separate influence of both  
18 forcing needs to be analysed more carefully to confirm this statement.  
19  
20  
21  
22  
23  
24  
25  
26  
27  
28  
29  
30

31 The influence of a possible large scale forcing was studied by Pingree and  
32 Le Cann (1989). Through numerical experiments, they obtained a circula-  
33 tion on the slope and the northern part of BoB shelf with the same current  
34 intensity and orientation as our observations. They explained this vertically  
35 averaged poleward circulation on the slope as a result of the combination  
36 of the large scale meridional density gradient and the steep slope known as  
37 the JEBAR term (Huthnance, 1984). On the northern part of the French  
38 continental slope, Pingree and Le Cann (1989) found a current intensity as-  
39 sociated with this term comparable to the observed circulation ( $\sim 5 \text{ cm s}^{-1}$ ).  
40 The shelf residual circulation is also poleward but the slope is too smooth  
41 to drive a JEBAR current comparable to our observations. The cross shelf  
42  
43  
44  
45  
46  
47  
48  
49  
50  
51  
52  
53  
54  
55  
56  
57  
58  
59  
60  
61  
62  
63  
64  
65

1  
2  
3  
4  
5 density gradient, as a consequence of the freshwater runoff from the French  
6 rivers (Lazure and Jegou, 1998), can also drive this poleward current but  
7 these runoffs strongly depend on the season. In the next section, we will  
8 discuss the influence of the wind forcing on the shelf circulation  
9

#### 10 11 12 13 *4.1.2. Seasonal Circulation* ★ 14

15 The seasonal averages show a relatively weak circulation over the upper  
16 slope and shelf of the BoB and important seasonal and geographical variabil-  
17 ities (figure 7). In winter, our results present tidally filtered current intensity  
18 up to about  $\sim 40 \text{ cm s}^{-1}$  at the surface of the Penmarc'h section at the 60  
19 m isobath while, in the 44°N section, strong currents occur in summer and  
20 autumn with a deep vertical extension. With the exception of these short  
21 strong current events in the 44°N section on each of instrumented isobaths,  
22 the near bottom circulation on the shelf of the BoB presents coherent flows  
23 over a large spatial scale. Indeed, current oscillations occur in the late win-  
24 ter and spring seasons with period of a month. For the rest of the year,  
25 the currents in the Loire section are correlated either with the 44°N section  
26 circulation or the Penmarc'h section circulation. It suggests a forcing over  
27 the same large spatial scale. The section 4.2 shows the influence of either  
28 local or remote winds on this circulation.  
29  
30  
31  
32  
33  
34  
35  
36  
37  
38  
39  
40  
41

42 The ASPEX data complements the near surface drifter data organized  
43 and described by Charria et al. (2011). Looking deeper in the water column,  
44 the main seasonal patterns of the surface circulation remain: strong and pole-  
45 ward autumnal currents, a weak shelf circulation in spring and equatorward  
46 currents in summer. However, some differences appear in winter where the  
47 currents recorded by the ADCP are strong and poleward all over the shelf  
48  
49  
50  
51  
52  
53  
54  
55  
56  
57  
58  
59  
60  
61  
62  
63  
64  
65

1  
2  
3  
4  
5 while the lack of information from drifters in the northern part of the BoB  
6 led to underestimate the circulation in this area. Because of the low strati-  
7 fication for this season, one can expect weak differences between the surface  
8 circulation and the interior flow. Thus, the weak circulation observed by  
9 drifters can be explained by less drifter data in winter or the inter-annual  
10 variability of the BoB circulation. The winter circulation of the BoBSS is fre-  
11 quently marked by a large scale poleward current off northern Spain (called  
12 "Navidad", Pingree (1994)). Garcia-Soto and Pingree (2012) observes in the  
13 last three decades (1979-2010) a marked Navidad, all along northern Spain,  
14 with an irregular periodicity of 2-6 years (3 years as mean with a standard  
15 deviation of  $\sim 1$  year). The most recent Navidad event occurred at the end of  
16 the year 2009 during the ASPEX project. This event most likely influences  
17 the strong and barotropic current event in the southern part of the BoBSS  
18 during the autumn season.  
19  
20  
21  
22  
23  
24  
25  
26  
27  
28  
29  
30

31 Our study also highlights the seasonality of the shelf circulation especially  
32 the seasonal differences between the summer circulation and the rest of the  
33 year. For this season, the mean vertically averaged currents present equator-  
34 ward currents on the shelf in front of the Loire river and close to the shelf  
35 break in the southern part of the BoB (figure 5). Along the 130 m isobath  
36 in Loire and 44°N sections, these equatorward currents are increasing from  
37 the bottom to the surface. At the 60 m isobath in front of the Loire river,  
38 we observe a marked vertical shear with equatorward currents at the surface  
39 and poleward currents at the bottom (figure 6). For this season, the south-  
40 eastward wind regime can drive the surface intensified equatorward flow but,  
41 it does not drive the entire deep circulation in the middle of the continental  
42  
43  
44  
45  
46  
47  
48  
49  
50  
51  
52  
53  
54  
55  
56  
57  
58  
59  
60  
61  
62  
63  
64  
65

1  
2  
3  
4 shelf in front of the Loire river. At this location, Vincent and Kurc (1969b)  
5 described a structure called "bourelet froid" (cold pool) which appears after  
6 the set up of the seasonal thermocline. This structure tends to drive a surface  
7 intensified cyclonic circulation in front of the Loire river (i.e. a poleward flow  
8 close to the coast) in the interior of the water column (Charria et al., 2011).  
9 Such cyclonic circulation around a cold pool has been observed in the Celtic  
10 and Irish sea (Hill, 1993).  
11

12  
13  
14  
15  
16  
17  
18 Another feature of the summer circulation is the shape of the vertical  
19 profiles of the cross-shore velocity component (figure 6). On the shelf, we ob-  
20 serve a weak or slightly offshore flow at the bottom while there is a markedly  
21 onshore current at the depth of the thermocline. This pattern has been ob-  
22 served along the western American coast (Lentz and Trowbridge, 2001) and  
23 over the Mid-Atlantic bight (Lentz, 2008). It fits with the theoretical frame  
24 of the Arrested Topographic Wave (ATW) (Csanady, 1978). An along-shore  
25 jet with shallow water on the right can drive a downslope current at the bot-  
26 tom in the Ekman layer. By continuity, it lead to an onslope interior flow.  
27 However, such patterns observed with an ADCP have to be analyzed care-  
28 fully because, in a region with enhanced internal waves activities (Pingree  
29 and New, 1989), the recorded time series could present strong biases at the  
30 thermocline depth. Indeed, an ADCP records the current velocities at fixed  
31 depths, thus, the velocities in the layers above and below the thermocline are  
32 recorded by the same cell because of the vertical displacement of the ther-  
33 mocline due to the presence of internal waves (Pingree and Le Cann, 1989).  
34 From the shelf break to the coast, it may leads to an increase of the observed  
35 mean cross-shore velocity in the direction of the phase speed propagation of  
36  
37  
38  
39  
40  
41  
42  
43  
44  
45  
46  
47  
48  
49  
50  
51  
52  
53  
54  
55  
56  
57  
58  
59  
60  
61  
62  
63  
64  
65



1  
2  
3  
4  
5 the internal wave because velocity field of internal waves above and below  
6 the thermocline are opposed (Phillips, 1977). The observed feature on the  
7 vertical profiles of the cross shore currents (figure 6) can be forced either by  
8 the ATW mechanism or the bias of an eulerian measurement in an internal  
9 waves field.

10  
11  
12 The internal wave can also influence the circulation at the 450 m isobath.  
13  
14 This isobath is approximatively the depth where internal wave are generated  
15 through the interaction with the topography. Internal wave beams are gener-  
16 ated at the shelf break and propagate downslope with an angle with the slope  
17 depending on the stratification at the generation location. These waves have  
18 strong spatial variability and the mean currents associated to these waves  
19 can reach  $\sim 15 \text{ cm s}^{-1}$  on the upper slope near "La Chapelle" bank (Pingree  
20 and Le Cann, 1989).  
21  
22  
23  
24  
25  
26  
27  
28  
29

#### 30 31 *4.2. Wind Driven circulation*

★

32  
33 The correlations between the local winds and the along-shore velocities  
34 ( $> 0.5$ ) suggest a strong influence of the wind on the circulation at the 60 m  
35 isobath but our results (figures 8 and 9) suggest two kinds of processes that  
36 occurs on the BoBSS. Indeed, the oriented time lagged correlations can be  
37 divided into two groups through both direction and time lag criteria.  
38  
39  
40  
41

42 On one hand, the observed along-shore circulation is well correlated with  
43 the along-shore wind and the time lags associated to this dynamics are ap-  
44 proximately twelve hours. The depth-averaged dynamics is primarily forced  
45 by the wind stress, along-shelf pressure gradient, and bottom stress (Lentz  
46 and Fewings, 2012). A simple frictional and barotropic model (Csanady,  
47 1982) assumes a timescale adjustment to wind forcing defined by  $T = H/r$   
48  
49  
50  
51  
52  
53

1  
2  
3  
4  
5 where  $T$  is the time scale adjustment,  $H$  is the water column height and  $r$   
6 the linear bottom friction. In the BoBSS,  $r$  is approximated as  $r = C_d|u_{tide}|$   
7 with  $C_d = 2.5 \times 10^{-3}$  a friction coefficient and  $|u_{tide}| = 0.5 \text{ m s}^{-1}$  an approx-  
8 imation of the tide current intensity. At the 60 m isobath and for a linear  
9 bottom friction  $r = 1.3 \times 10^{-3} \text{ m s}^{-1}$ , we obtain a time scale adjustment of  
10 12 hours. It can be compared to the time lags we observe in the BoBSS.  
11

12  
13  
14  
15  
16 On the other hand, at  $44^\circ\text{N}$ , the observed along-shore circulation is well  
17 correlated with westerlies and the time lags associated to this dynamics are  
18 longer than a day. This suggests local along-shore currents forced by remote  
19 winds. Such a mechanism implies a longer time lag (Lentz and Fewings,  
20 2012) than for a mechanism where the along-shore currents are driven by the  
21 local along-shore winds. Batifoulier et al. (2012) described the circulation  
22 in the southern part of the BoB as influenced by the north Spanish coast  
23 circulation for summer and autumn. For these seasons, the stratification is  
24 strong and the westerlies drive a downwelling circulation. The adjustment  
25 of the thermocline to the wind generates baroclinic waves associated with  
26 strong current events. In this study, ASPEX data suggest that the southern  
27 part of the BoB is influenced by the north Spanish coast circulation during  
28 the whole year.  
29  
30  
31  
32  
33  
34  
35  
36  
37  
38  
39  
40

41 Some correlation points in the Penmarc'h section do not fit with either  
42 the frictional model or the remote wind forcing explanation. For spring and  
43 summer in this section, the correlation points are aligned with the local along-  
44 shore direction with values of 0.4 and time lags about 2-3 days. This indicates  
45 a weak driving influence of the along-shore winds on the local circulation.  
46  
47  
48  
49  
50 This also strongly suggests that some other mechanisms are able to force the  
51  
52  
53  
54  
55  
56  
57  
58  
59  
60  
61  
62  
63  
64  
65

1  
2  
3  
4  
5 main part of the circulation in this section. These other mechanisms may  
6 be the driving mechanisms of the  $\sim 40\%$  of the observed circulation which  
7 are not explained by the wind forcing in the other sections. The section  
8  
9  
10  
11 5 discusses these driving mechanisms by comparing the circulation observed  
12 during the ASPEX project with the well documented area of the Mid Atlantic  
13 Bight.  
14  
15

## 16 17 18 **5. Conclusion** 19

20 The circulation in the Bay of Biscay is estimated at 10 locations with ob-  
21 servations throughout the water column along three sections from the coast  
22 to the upper slope at 60 m, 130 m and 450 m isobaths . The nearly two  
23 year time series are used to describe the mean circulation and its temporal  
24 evolution as an eastern ocean boundary circulation. The depth and season-  
25 ally averaged currents are poleward throughout the Bay of Biscay except in  
26 summer on the shelf in front of the Loire river where the currents can be  
27 equatorward. The seasonal variability of these currents is constrained by to-  
28 pography and is weaker on the 130 m isobath. On the slope, the cross-shore  
29 currents are slightly downslope from mid-depth to the near bottom. On the  
30 shelf, the near bottom flow is also offshore but in the interior the vertical  
31 profiles present a greater variability likely due to the wind, the cross-shore  
32 gradient density and likely some bias due to the Eulerian measurement of  
33 internal waves activity. The temporal evolution of the circulation presents  
34 strong barotropic events observed at 60 m depth during the summer and  
35 autumn seasons in the south of the Bay of Biscay. And in winter, the circu-  
36 lation in the north is characterized by a strong surface intensified variability.  
37  
38  
39  
40  
41  
42  
43  
44  
45  
46  
47  
48  
49  
50  
51  
52  
53

1  
2  
3  
4  
5 At the bottom, oscillations of the weekly averaged current can be observed  
6 throughout the Bay of Biscay shelf and slope in winter.  
7

8  
9 The Bay of Biscay shelf and slope circulation may be mainly driven by  
10 large scale along-shore pressure gradient, cross-shore buoyancy gradients and  
11 the local winds. The data from the ASPEX experiment provides good prox-  
12 ies to separate each of the forcing mechanisms. In our study, a first step is  
13 performed estimating the wind driven circulation. At the coast, the wind  
14 driven circulation is about 60% of the total circulation. Locally, in the Pen-  
15 marc'h and Loire river sections, the variability of the along-shore currents is  
16 driven by the along-shore winds with a spin up time around 10 hours. In the  
17 44°N section the circulation is likely indirectly driven by the wind blowing  
18 along the Spanish coast. Here, the influence of the wind is lagged in time  
19 because the currents are possibly remotely forced through coastal trapped  
20 wave propagation. The repetition of strong current events from a year to  
21 another indicates that the circulation in the French part of the Bay of Biscay  
22 shelf and slope seems to be consistent in time despite the changes in the  
23 atmospheric forcing and/or the presence or absence of a Navidad current.  
24  
25  
26  
27  
28  
29  
30  
31  
32  
33  
34  
35  
36  
37

38 *Acknowledgment.* This work is part of the EPIGRAM project supported by  
39 the Agence Nationale de la Recherche (grant ANR-08-BLAN-0330-01) and  
40 CNRS/INSU national programme LEFE/IDAO. Special thanks are due to  
41 the institutes that provided the data for this study: IFREMER, Météo-  
42 France. The authors would like to thank the technical staff who worked on  
43 the preparation, deployment and the recovery of the instruments.  
44  
45  
46  
47  
48  
49  
50  
51  
52  
53  
54  
55  
56  
57  
58  
59  
60  
61  
62  
63  
64  
65

## Appendix A. Wind stress

Many formula for the wind stress computation have been proposed (Geernaert, 1987). For this study, we take the wind stress formulation from Smith and Banke (1975):

$$C_s = 0.63 + 0.066|u_{10}^{\vec{}}| \quad (\text{A.1a})$$

$$\vec{\tau} = \rho_a C_s |u_{10}^{\vec{}}| u_{10}^{\vec{}} \quad (\text{A.1b})$$

$u_{10}^{\vec{}}$  is the wind vector measured at 10 m above the sea level,  $\rho_a$  is the air density ( $\rho_a = 1.2 \text{ kg.m}^{-3}$ ) and  $C_s$  the drag coefficient.

## References

- M.A. Al-Zanaidi, B.D. Dore, 1976. Some Aspects of Internal Wave Motions. *Pure and Applied Geophysics* 3 (14), 403–414.
- Batifoulier, F., Lazure, P., Bonneton, P., 2012. Poleward coastal jets induced by westerlies in the Bay of Biscay. *Journal of Geophysical Research* 117 (C3), 1–19.
- Beardsley, R., Winant, C., 1979. On the Mean Circulation in the Mid Atlantic Bight. *Journal of Physical Oceanography* 9, 612–619.
- Björnsson, H., Venegas, S., 1997. A manual for EOF and SVD analyses of climate data. Report. No 97-1, Department of Atmospheric and Oceanic Sciences and Centre for Climate and Global Change Research, McGill University. 52.

- 1  
2  
3  
4  
5 Brown, J., Carrillo, L., Fernand, L., Horsburgh, K., A.E Hill, Young, E.,  
6 Medler, K., 2003. Observations of the physical structure and seasonal jet-  
7 like circulation of the Celtic Sea and St. George's Channel of the Irish Sea.  
8 Continental Shelf Research 23 (6), 533–561.  
9
- 10  
11  
12  
13 Chapman, D. C., Beardsley, R., 1989. On the Origin of Shelf Water in the  
14 Middle Atlantic Bight. Journal of Physical Oceanography 3, 384–391.  
15  
16  
17  
18 Charria, G., Lazure, P., Le Cann, B., Serpette, A., Reverdin, G., Louazel, S.,  
19 Batifoulier, F., Dumas, F., Pichon, A., Morel, Y., Oct. 2011. Surface layer  
20 circulation derived from Lagrangian drifters in the Bay of Biscay. Journal  
21 of Marine Systems, in press,doi:10.1016/j.jmarsys2012.09.015  
22  
23  
24  
25  
26 Csanady, G. T., 1978. The Arrested Topographic Wave. Journal of Physical  
27 Oceanography 8, 47–62.  
28  
29  
30  
31 Csanady, G. T., 1982. Circulation in the Coastal Ocean, Springer's Edition.  
32 Vol. 2687. D. Reidel Publishing Company.  
33  
34  
35  
36 Déqué, M., Dreveton, C., Braun, A., Cariolle, D., 1994. The ARPEGE/IFS  
37 atmosphere model: a contribution to the French community climate mod-  
38 elling. Climate Dynamics, 249–266.  
39  
40  
41  
42 Ferrer, L., Fontán, A., Mader, J., Chust, G., González, M., Valencia, V.,  
43 Uriarte, A., Collins, M., Apr. 2009. Low-salinity plumes in the oceanic  
44 region of the Basque Country. Continental Shelf Research 29 (8), 970–984.  
45  
46  
47  
48  
49 Garcia-Soto, C., Pingree, R.D., 2012. Atlantic Multidecadal Oscillation  
50 (AMO) and sea surface temperature in the Bay of Biscay and adjacent  
51  
52  
53  
54  
55  
56  
57  
58  
59  
60  
61  
62  
63  
64  
65

1  
2  
3  
4 regions. *Journal of the Marine Biological Association of the United King-*  
5 *dom* 92(2), 213–234.  
6  
7

8  
9 Geernaert, G., 1987. On the importance of the drag coefficient in air-sea  
10 interactions. *Dynamics of Atmospheres and Oceans* 11, 19–38.  
11  
12

13 Godin, G., 1972. *The Analysis of Tide*, University of Toronto Press, 264 pp.  
14  
15

16 Hill, A.E., 1993. Seasonal Gyre in Shelf Seas. *Annales Geophysicales-*  
17 *Atmosphere Hydrospheres and Space* 11 (11-12), 1130–1137.  
18  
19

20 Holloway, G., 1992. Representing Topographic Stress for Large-Scale Ocean  
21 Models. *Journal of Physical Oceanography* 22 (9), 1033–1046.  
22  
23

24 Houghton, R., Schlitz, R., Beardsley, R., Butman, B., Chamberlin, J., 1982.  
25 Middle Atlantic Bight cold pool: Evolution of the temperature structure  
26 during summer 1979. *Journal of Physical Oceanography* 12 (10), 1019–  
27 1029.  
28  
29  
30  
31  
32

33 Huthnance, J. M., 1984. Slope Currents and "JEBAR". *Journal of Physical*  
34 *Oceanography* 14, 795–810.  
35  
36  
37

38 Isemer, H., Hasse, L., 1987. *The Bunker climate atlas of the North Atlantic*  
39 *Ocean. Volume II: Air-sea interactions, Springer-Verlag Edition. Vol. II.*  
40  
41  
42

43 Koutsikopoulos, C., Le Cann, B., 1996. Physical processes and hydrological  
44 structures related to the Bay of Biscay anchovy. *Scientia Marina* 60, 9–19.  
45  
46  
47

48 Lazare, P., Dumas, F., Vrignaud, C., Jul. 2008. Circulation on the Armorican  
49 shelf (Bay of Biscay) in autumn. *Journal of Marine Systems* 72 (1-4), 218–  
50 237.  
51  
52  
53

- 1  
2  
3  
4  
5 Lazure, P., Jegou, A.M., 1998. 3D modelling of seasonal evolution of Loire  
6 and Gironde plumes on Biscay Bay continental shelf. *Oceanologica Acta*  
7 21 (2), 165–177.  
8  
9
- 10  
11 Le Cann, B., 1982. Evolution annuelle de la structure hydrologique du  
12 Plateau Continental au sud de la Bretagne. Ph.D. thesis, Université de  
13 Bretagne Occidentale.  
14  
15  
16  
17  
18 Le Cann, B., 1988. Dépouillement des données de courants, de températures  
19 et d'hydrologie (03/03/198724/04/1987), CIRESOL. Tech. rep., Université  
20 de Bretagne Occidentale.  
21  
22  
23  
24  
25 Lentz, S., Trowbridge, J., 2001. A Dynamical Description of Fall and Win-  
26 ter Mean Current Profiles over the Northern California Shelf. *Journal of*  
27 *Physical Oceanography* 31 (4), 914–931.  
28  
29  
30  
31  
32 Lentz, S. J., Jul. 2008. Seasonal Variations in the Circulation over the Middle  
33 Atlantic Bight Continental Shelf. *Journal of Physical Oceanography* 38 (7),  
34 1486–1500.  
35  
36  
37  
38  
39 Lentz, S. J., Fewings, M. R., 2012. The Wind- and Wave-Driven Inner-Shelf  
40 Circulation. *Annual Review of Marine Science* 4 (1), 317–343.  
41  
42  
43  
44  
45 Michel, S., A.M. Treguier, Vandermeirsch, F., 2009. Temperature variability  
46 in the Bay of Biscay during the past 40 years, from an in situ analysis and  
47 a 3D global simulation. *Continental Shelf Research* 29 (8), 1070–1087.  
48  
49  
50  
51  
52 Phillips, O.M, 1977. *The Dynamics of the upper ocean*. Cambridge University  
53 Press, London.  
54  
55  
56  
57  
58  
59  
60  
61  
62  
63  
64  
65



- 1  
2  
3  
4  
5 Pingree, R., Sinha, B., Griffiths, C.R., 1999. Seasonality of the European  
6 slope current (Goban Spur) and ocean margin exchange.. *Continental Shelf*  
7 *Research* 19 (7), 929–975.  
8  
9  
10  
11 Pingree, R., 1994. Winter Warming in the southern Bay of Biscay and la-  
12 grangian eddy kinematics from a deep drogued ARGOS buoy. *Journal of*  
13 *the Marine Biological Association of the United Kingdom* 74, 107–128.  
14  
15  
16  
17 Pingree, R., 1993. Flow of surface waters to the west of the British Isles  
18 and in the Bay of Biscay. *Deep Sea Research Part II: Topical Studies in*  
19 *Oceanography* 40 (1-2), 369–388.  
20  
21  
22  
23  
24 Pingree, R., Le Cann, B., 1989. Celtic and Armorican slope and shelf residual  
25 currents. *Progress In Oceanography* 23 (4), 303–338.  
26  
27  
28  
29 Pingree, R. D., Le Cann, B., 1990. Structure, strength and seasonality of the  
30 slope currents in the Bay of Biscay region. *Journal of the Marine Biological*  
31 *Association of the United Kingdom* 70 (04), 857–885.  
32  
33  
34  
35  
36 Pingree, R. D., Le Cann, B., 1992. Three anticyclonic Slope Water Oceanic  
37 eDDIES (SWODDIES) in the Southern Bay of Biscay in 1990. *Deep-Sea*  
38 *Research* 39 (718), 1147–1175.  
39  
40  
41  
42  
43 Pingree, R. D., New, A. L., 1989. Downward propagation of internal tidal  
44 energy into the Bay of Biscay. *Deep Sea Research Part A. Oceanographic*  
45 *Research Papers* 36 (5), 735–758.  
46  
47  
48  
49  
50  
51  
52  
53  
54  
55  
56  
57  
58  
59  
60  
61  
62  
63  
64  
65

- 1  
2  
3  
4  
5 Puillat, I., Lazure, P., Jégou, A., Lampert, L., Miller, P., 2004. Hydrograph-  
6 ical variability on the French continental shelf in the Bay of Biscay, during  
7 the 1990s. *Continental Shelf Research* 24 (10), 1143–1163.  
8  
9  
10  
11 Semtner, A., Mintz, Y., 1977. Numerical Simulation of the Gulf Stream and  
12 Mid-Ocean Eddies. *Journal of Physical Oceanography* 7, 208–230.  
13  
14  
15  
16 Smith, S. D., Banke, E. G., 1975. Variation of the sea surface drag coefficient  
17 with wind speed. *Quarterly Journal of the Royal Meteorological Society*  
18 101 (429), 665–673.  
19  
20  
21  
22  
23 Somavilla, R., González-Pola, C., Lavín, a., Rodriguez, C., 2012.  
24 Temperature and salinity variability in the south-eastern corner of  
25 the Bay of Biscay (NE Atlantic). *Journal of Marine Systems*,in  
26 press,doi:10.1016/j.jmarsys.2012.02.010  
27  
28  
29  
30  
31 Van Aken, H. M., 2002. Surface currents in the Bay of Biscay as observed  
32 with drifters between 1995 and 1999. *Deep-Sea Research* 49, 1071–1086.  
33  
34  
35  
36 Vincent, A., Kurc, G., 1969a. Les Variations de la Situation Thermique dans  
37 le Golfe de Gascogne et leur incidence sur l'écologie et la pêche de la sardine  
38 en 1968. *Trav.Inst.Pêches maritimes* 33 (2), 203–212.  
39  
40  
41  
42 Vincent, A., Kurc, G., 1969b. Variations Saisonnières de la Situation Ther-  
43 mique du Golfe de Gascogne en 1967. *Rev.Trav.Inst.Pêches maritimes*  
44 33 (1), 79–96.  
45  
46  
47  
48  
49  
50  
51  
52  
53  
54  
55  
56  
57  
58  
59  
60  
61  
62  
63  
64  
65